

# **A ~~531406~~-year non-growth—growing season precipitation reconstruction in the southeastern Tibetan Plateau**

Maierdang Keyimu<sup>1</sup>, Zongshan Li<sup>1\*</sup>, Bojie Fu<sup>1</sup>, Guohua Liu<sup>1</sup>, Weiliang Chen<sup>1</sup>, Zexin ~~Fan~~<sup>3</sup>Fan<sup>2</sup>, Keyan ~~Fang~~<sup>4</sup>Fang<sup>3</sup>, Xiuchen ~~Wu~~<sup>2</sup>Wu<sup>4</sup>, Xiaochun Wang<sup>5</sup>

<sup>1</sup>State Key Laboratory of Urban and Regional Ecology, Research Center for Eco-Environmental Sciences, Chinese Academy of Sciences, Beijing 100085, China

~~<sup>2</sup>Xishuangbanna Tropical Botanical Garden, Chinese Academy of Sciences, Mengla 666303, China~~

~~<sup>2</sup>State Key Laboratory of Earth Surface Processes and Resource Ecology, Beijing Normal University, Beijing 100875, China~~

~~<sup>3</sup>Key Laboratory of Humid Subtropical Eco-Geographical Process (Ministry of Education), College of Geographical Sciences, Fujian Normal University, Fuzhou 350007, China~~

~~<sup>4</sup>State Key Laboratory of Earth Surface Processes and Resource Ecology, Beijing Normal University, Beijing 100875, China~~

~~<sup>3</sup>Xishuangbanna Tropical Botanical Garden, Chinese Academy of Sciences, Mengla 666303, China~~

~~<sup>4</sup>Key Laboratory of Humid Subtropical Eco-Geographical Process (Ministry of Education), College of Geographical Sciences, Fujian Normal University, Fuzhou 350007, China~~

<sup>5</sup>College of Forestry, Northeast Forestry University, Harbin 150040, China

Correspondence to: Zongshan Li (zsl\_i\_st@rcees.ac.cn)

**Abstract.** Trees record climatic conditions during their growth, and tree-rings serve as a proxy to reveal the features of the historical climate of a region. In this study, we collected tree-ring cores of forest hemlock (*Tsuga forrestii*) from the northwestern Yunnan area of the southeastern Tibetan Plateau (SETP), and created a residual tree-ring width (TRW) chronology. An analysis of the relationship between tree growth and climate revealed that precipitation during the non-growth growing season (NGS) (from November of the previous year to February of the current year) was the most important constraining factor on the radial tree growth of forest hemlock in this region. In addition, the influence of NGS precipitation on radial tree growth was relatively uniform over time (1956–2005). Accordingly, we reconstructed the NGS precipitation over the period spanning from A.D. ~~4475~~1600–2005. The reconstruction accounted for 28.5% of the actual variance during the common period 1956–2005, and the leave-one-out verification parameters indicated the reliability of the reconstruction. Based on the reconstruction, NGS was extremely dry during the years A.D. ~~4475~~–1656, 1670, 1694, 1703, 1736, 1897, 1907, 1943, 1969, 1982, and 1999. In contrast, the NGS was extremely wet during the years A.D. ~~4491~~–1536, ~~1558~~–1627, 1638, 1654, 1832, 1834–1835, and 1992. Similar variations of the NGS precipitation reconstruction series and Palmer Drought Severity Index (PDSI) reconstructions of early growing season from surrounding regions indicated the reliability of the present

30 reconstruction. A comparison of the reconstruction with Climate Research Unit (CRU) gridded data revealed that our  
31 reconstruction was representative of the NGS precipitation variability of a large region in the SETP.

32 **Keywords:** Tree-rings; [Winter-Non-growing season](#) precipitation; Reconstruction; Southeastern Tibetan Plateau

### 33 1 Introduction

34 Unravelling the past climate often relies on proxy records. As a widely used proxy material, tree-rings provide an opportunity  
35 to obtain long-term climate data (Fritts, 1976; Esper et al., 2002; D'Arrigo et al., 2005; Li et al., 2011; Büntgen et al., 2011,  
36 2016; Cai et al., 2014; Yang et al., 2014; Schneider et al., 2015; Wilson et al., 2016; Keyimu et al., 2021). These long-term  
37 records enable us to identify the inter-annual, decadal and multi-decal variability of historical climatic conditions. They also  
38 provide a reference to better understand the nature of current climatic conditions (warming/cooling, drying/wetting) and to  
39 project the future regional climate, as well as the dynamic response of earth processes (e.g., forest growth, glacier  
40 retreat/advance, stream flow, drought frequency, and forest fires) to climate change.

41 Being the “third pole” of the [planet](#) Earth, the Tibetan Plateau (TP) (average 4000 m a.s.l.) is particularly sensitive to climate  
42 change and is one of the fastest warming places in the world (Chen et al., 2020). The average decadal temperature increase at  
43 the TP is 0.33°C, which is higher than the world’s average decadal temperature increase of 0.20°C (Yan and Liu, 2014).  
44 Because of its geographical extent and position within the global circulation system, the TP plays a key role in regional and  
45 global atmospheric circulation patterns (Griessinger et al., 2017), not only affecting the mid-latitude westerlies, but also  
46 influencing the Asian monsoon circulation through its thermo-dynamical feedbacks (Duan et al., 2006; Rangwala, 2009; Wu  
47 et al., 2015).

48 There are large areas of coniferous forest distributed at high altitudes in the southeastern Tibetan Plateau (SETP). Due to  
49 their age and relative lack of disturbance they are a source of proxy material (tree-rings) that can be used to reveal the past  
50 climatic conditions in this region (Bräuning and Mantwill, 2004; Griessinger et al., 2017; Fan et al., 2009; Fang et al., 2010;  
51 Li et al., 2011; Wang et al., 2015; Li and Li., 2017; Shi et al., 2017; Huang et al., 2019; Shi et al., 2019; Keyimu et al., 2021).  
52 Many dendroclimatological reconstructions of hydroclimatic variables have also been conducted in the SETP (Fan et al., 2008;  
53 Zhang et al., 2015; [Wernicke et al., 2015](#); [Griessinger et al., 2017](#); Li et al., 2017; He et al., 2018). However, few studies have  
54 focused on the reconstruction of precipitation history (He et al., 2012). The non-growing season (NGS) of vegetation (from  
55 November of the previous year to February of the current year) includes the non-monsoon and pre-monsoon seasons in the  
56 SETP, and water availability during the NGS might therefore have a constraining effect on radial tree growth (Linderholm and  
57 Chen, 2005). It is important to understand the long-term precipitation variations during the NGS to evaluate the current trend  
58 of precipitation variation and estimate its future patterns, and to determine the future responses of the forest ecosystem under

59 the changing precipitation trend. To our knowledge, however, there have been no reports of the reconstruction of NGS  
60 precipitation in this area. This hinders our understanding of NGS variability from a long-term perspective.

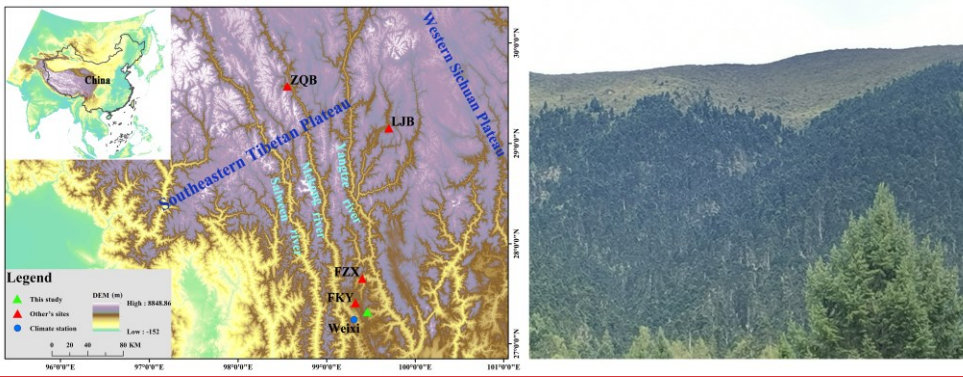
61 In this study, we collected tree-ring cores of forest hemlock from the Xinzhu Village of northwestern Yunnan in the SETP.  
62 The main objectives of the present study were to (1) identify the relationship between the radial growth of forest hemlock and  
63 climate, (2) reconstruct the regional precipitation history, and (3) validate the reliability of the reconstruction. Our results not  
64 only improve the historical precipitation information available in the SETP, but also provide the basis to evaluate the current  
65 trend of regional NGS precipitation variation, as well as the future development of regional forest growth.

## 66 **2 Materials and methods**

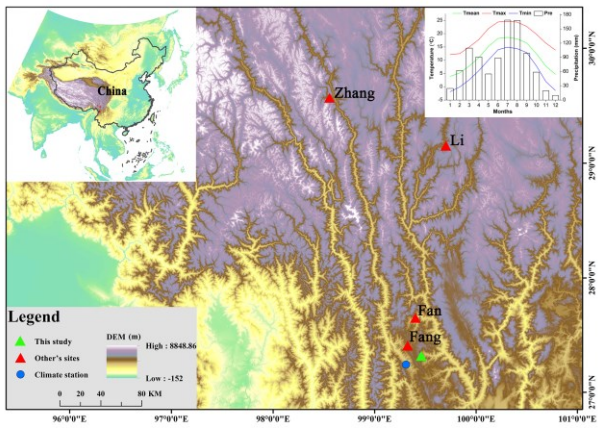
### 67 **2.1 Study area and sampling sites**

68 Tree-ring core samples were collected from Xinzhu Village in Lijiang County in northwestern Yunnan. The sample site was  
69 in the Hengduan Mountains in the SETP (Fig. 1). The climate of the study area is regulated by a westerly circulation and the  
70 monsoon circulations of the Indian and Pacific oceans. “Hengduan” means “transverse” in the Chinese language, which implies  
71 that the mountains in this region lie in the transverse direction from south to north, and the area is a passageway for the Indian  
72 monsoon to flow in and climb up to the TP and other parts of the mainland. The SETP is susceptible to monsoon flow and  
73 atmospheric circulations (Bräuning and Mantwill, 2004). According to the Weixi meteorological station of the China  
74 Meteorological Administration, which was the closest station to our sampling site, the mean annual precipitation was 953 mm  
75 from 1955 to 2016. Most of the annual precipitation (Nearly 70%) concentrated in the monsoon season from May to October  
76 in this region, and thus, tree growth is usually constrained by water availability during non-growing~~th~~ season. The coldest  
77 temperature was 3.9°C in January and the warmest temperature was 18.6°C in July. Tree-ring cores of forest hemlock were  
78 collected at a site that had not been impacted by anthropogenic disturbances. The elevation of the sampling site was 2,966 m  
79 a.s.l. A total of 48 tree-ring cores were extracted from 48 trees using a 5.1 mm diameter increment borer. We have used one  
80 sampling per tree method to improve the spatial representativity of radial tree growth. Sampling was conducted along an axis  
81 perpendicular to the slope inclination to avoid the impact of tension wood (Keyimu et al., 2020).

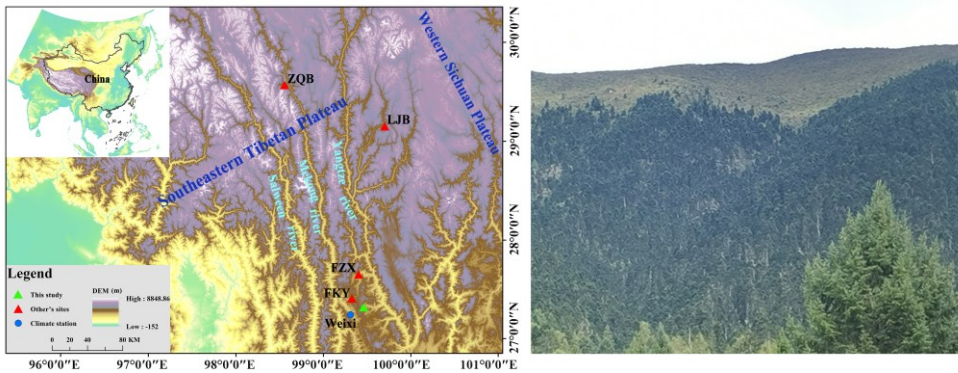
82



83



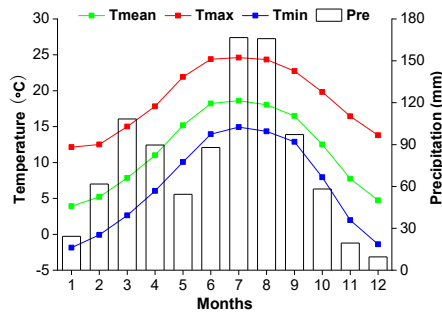
带格式的: 两端对齐



84

85 **Figure 1:** Map of the study area. The green triangle is the study site. The red triangles are the sites used in other studies (previous year May  
 86 – current year April PDSI reconstruction site in Fang et al., 2010; current year March – May PDSI reconstruction site in Fan et al., 2008;  
 87 current year April – June PDSI reconstruction site in Li et al., 2017; current year May - June PDSI reconstruction site in Zhang et al., 2015).  
 88 The blue dot is the meteorological station in Weixi County. On the right is the landscape image of tree ring sampling site. The figure at upper  
 89 right position is the ombrothermic diagram of the climate variables in the study area.

90



91

92 **Figure 2:** The figure at upper right position is the ombrothermic diagram of the climate variables in the study area.

## 93 2.2 Establishment of the tree-ring chronology

94 The tree-ring samples were treated with standard dendrochronological procedures. They were first glued onto wooden holders  
 95 and air-dried, and then polished to a flat surface with sand paper until the tree\_rings were clearly visible. The LINTAB 6.0

设置了格式: 字体: 非加粗, 复杂文种字体: 非加粗

设置了格式: 字体: 非加粗, 复杂文种字体: 非加粗

带格式的: 居中

设置了格式: 字体: 加粗, 复杂文种字体: 加粗

带格式的: 正文, 行距: 单倍行距

96 tree-ring measurement system was used to measure the tree-ring width (TRW). Crossdating was conducted visually by  
97 marking each sample at each ten-year interval, and then its quality was confirmed using the COFFECHA program (Holmes,  
98 1983). Thirty-eight of the tree-ring cores were adopted for a further analysis after excluding the bad quality samples and the  
99 un-crossdated samples. The tree-ring series was detrended with a negative exponential model to remove the age dependency  
100 of tree growth (Cook et al., 1995). We have used the residual chronology since it removes the auto-correlation in tree-ring  
101 growth and captures high frequent climate signal. The “dplR” software toolkit (Bunn, 2018) within the R software environment  
102 (R Core Team 2019/2020) was used for detrending and chronology establishment. The reliable period of the chronology was  
103 determined based on the criterion of expressed population signal (EPS) > 0.85 (Wigley, 1984).

### 104 2.3 Climate data

105 Temperature and precipitation records were obtained from the Weixi meteorological station (27.17° N, 99.28° E, 2326 m  
106 a.s.l.) operated by the China Meteorological Administration. Data was available for the period of 1955–2005. Climate data  
107 (including the maximum, minimum and average temperatures, and precipitation) were provided by the China Meteorological  
108 Data Sharing Service Platform. A self-calibrated Palmer Drought Severity Index (scPDSI) was downloaded from the 3.26e  
109 gridded dataset of the Climate Research Unit (CRU) via the Royal Netherlands Meteorological Institute (KNMI) climate  
110 explorer (data accessed on 23<sup>rd</sup> December, 2020, [data re-accessed for the updated version \(CRU scPDSI 4.05 early\) of PDSI](#)  
111 [data on 20<sup>th</sup> of April, 2021](#)) using the coordinates of the tree-ring sampling site. The range of CRU grid box is 27.0 – 27.5° N,  
112 99.0 – 99.5° E.

### 113 2.4 Tree growth and climate relationship analysis

114 We analysed the relationship between climate and tree growth using Dendroclim 2002 software (Biondi and Waikul, 2004).  
115 Pearson correlation values and response function values were calculated for the relationships between TRW indices and climate  
116 variables for the period of 1955–2005. Due to the carry over effect of the climatic conditions of the previous-year on the current  
117 year tree growth (Fritts, 1976), the tree growth – climate relationship analysis spanned a 16-month period from June of the  
118 previous year to September of the current year. We also used the seasonalised climate variables because it made more eco-  
119 physiological sense for growth than single months. To observe the temporal stability of the climate influence on radial tree  
120 growth, we conducted a moving correlation analysis at a moving interval of 32 years. All the correlation results were considered  
121 significant at the 95% confidence level.

### 122 2.5 Climate reconstruction

123 According to the analysis of the relationship between the TRW indices and constraining climatic factors, we developed a linear  
124 regression model (Cook and Kairiukstis, 1990) for the climate reconstruction. As in many other tree-ring based climate  
125 reconstructions, we tested the goodness-of-fit of the model using the leave-one-out cross-validation method (Michaelsen, 1987).

设置了格式: 字体:(默认)+西文标题 (Times New Roman), 复杂文  
种字体:+西文标题 (Times New Roman)

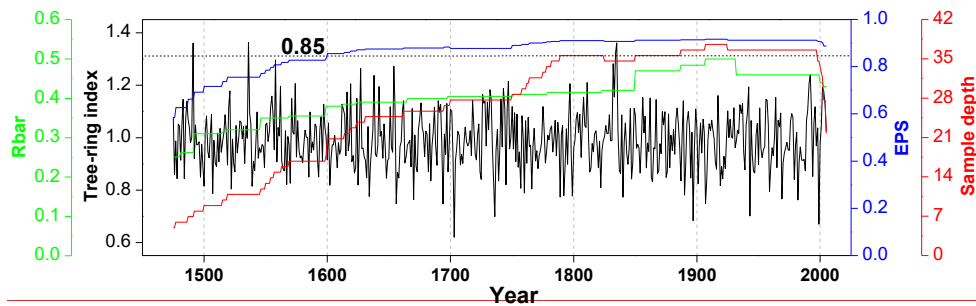
设置了格式: 上标

126 We used the Pearson's correlation coefficient ( $r$ ), explained variance ( $R^2$ ), adjusted explained variance ( $R_{adj}^2$ ), reduction of  
127 error (RE), sign test (ST), coefficient of efficiency (CE) and product mean test (Pmt) and Durbin-Watson test (DW) to evaluate  
128 the fidelity of the reconstruction model (Fritts et al., 1990).

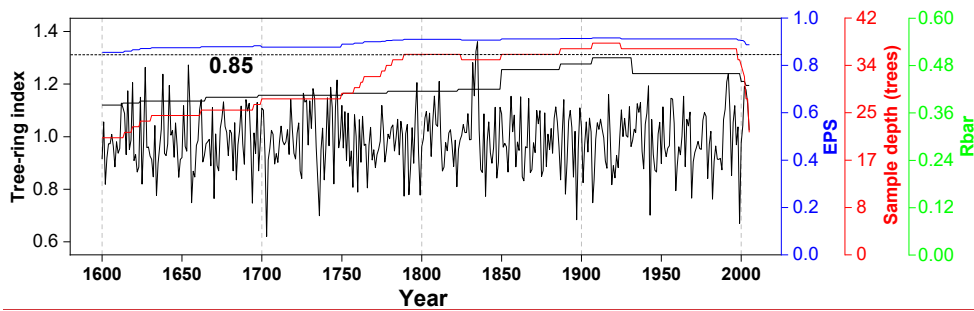
### 129 3. Results

#### 130 3.1 Characteristics of the TRW chronology

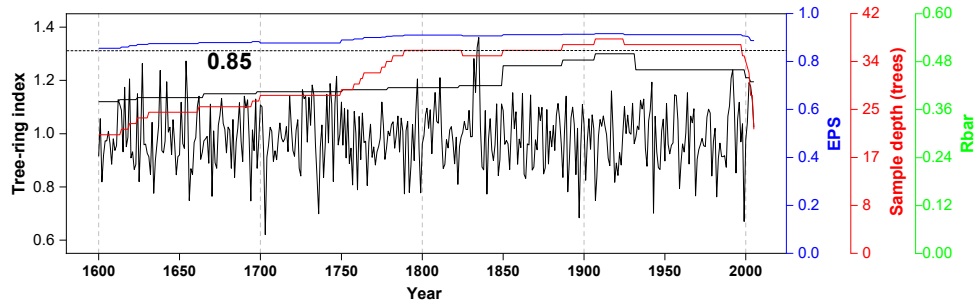
131 Residual TRW chronology of forest hemlock from the investigation area was established (Fig. 23). The descriptive statistics  
132 of the chronology were presented in Table 1. According to the criteria of  $EPS > 0.85$ , the most reliable length of the TRW  
133 chronology was 405–406 years (A.D. 1600–2005). The EPS value of the chronology over the period of A.D. 1475–1600 was  
134 below 0.85. The mean correlation among tree-ring series ( $R_{bar}$ ) was 0.4748, and the variance in the first eigenvector (VFE)  
135 was 26–27 %, which implied a relatively strong common signal among individual trees constituting the chronology. The  
136 relatively low inter-annual variability of the chronology was expressed by the small mean sensitivity value (0.2423). The EPS  
137 and SNR values (average EPS and SNR were 0.8689 and 5.99687 for the total length chronology, respectively) further implied  
138 the existence of the common signal among each individual measurement series. In general, all the statistical parameters  
139 indicated the potential climate signal imprinted in our TRW chronology.



140



141



142

143 **Figure 32:** Plot of tree-ring residual chronology, the running inter-correlations among cores (Rbar, the green line), expressed population  
 144 signal (EPS, the blue line) and the sample size (the red line). The Rbar and EPS were calculated using a 30-year window, with a 15-year lag.  
 145 The horizontal dashed line denotes the EPS threshold level (0.85).

146

147 **Table 1.** Site information, chronology statistics and results of a common interval span analysis of residual tree-ring width  
 148 (TRW) chronology from the Xinzhu Village, northwestern Yunnan in China

Type	Location	Elevation (m)	Time length	Number of cores	SD	MS	Rbar	SNR	EPS	VFE
Tree ring	99.43°E, 27.25°N	2966	1475-1600- 2005	38	0.2322	0.234	0.487	6.875- 99	0.896	0.276

149 **Note:** SD: standard deviation, MS: mean sensitivity, Rbar: mean inter-series correlation, SNR: signal-to-noise ratio, EPS: Expressed  
 150 Population Signal, VFE: Variance in first eigenvector.

设置了格式: 字体: 非加粗, 复杂文种字体: 非加粗

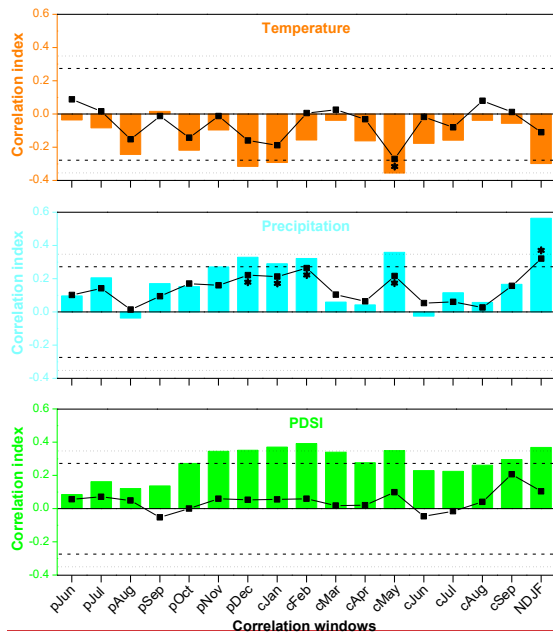
设置了格式: 字体: 非加粗, 复杂文种字体: 非加粗

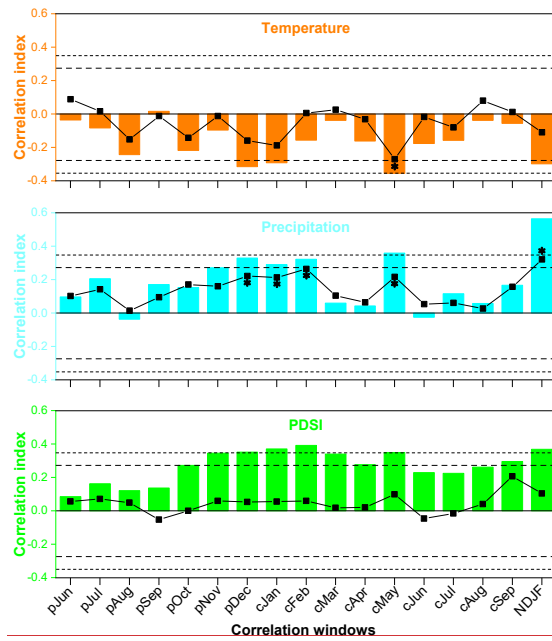
设置了格式: 字体: 非加粗, 复杂文种字体: 非加粗

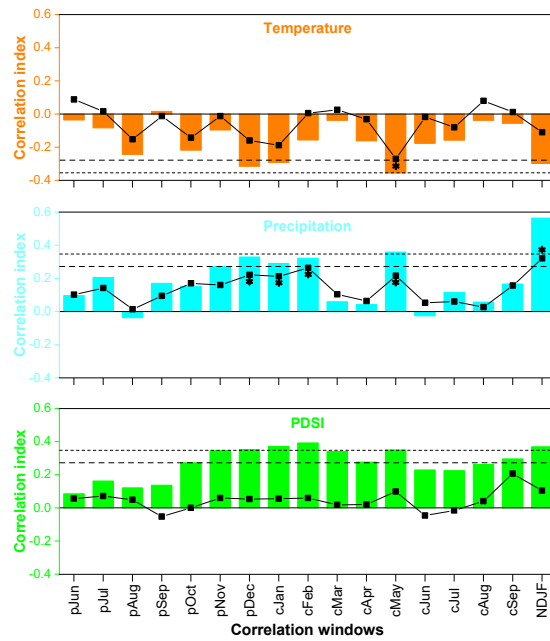


151 **3.2 Tree growth and climate relationship analysis**

152 According to the results of the tree growth and climate relationship analyses (Fig. 34), the precipitation during the NGS was  
153 the most important constraining factor ( $R = 0.56$ ,  $p < 0.001$ ) on the radial growth of forest hemlock in the study area. The  
154 results of a response function analysis further confirmed the strong correlation between NGS precipitation and forest hemlock  
155 radial growth. The results of a moving correlation analyses between TRW chronology and instrumental NGS precipitation  
156 record (Fig. 45) were positively significant (at 99%) during the investigated period (1956-2005), indicating that the NGS  
157 precipitation influence was stationary over time.





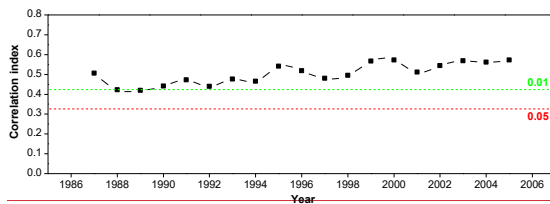


160

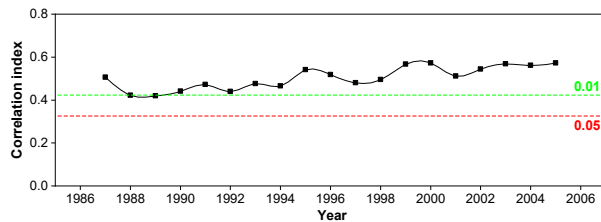
161 **Figure 43.** Correlations between tree-ring indices and temperature, precipitation, and scPDSI in the correlation windows from  
 162 previous year June to current year September, as well as in NDJF (non-growing season, NGS) for the common period from  
 163 1956 to 2005. The horizontal dashed and dotted lines indicate the threshold of the correlations at the 95% and 99% significance  
 164 levels. Black line with squares denotes the results of response function analysis between tree-ring indices and climate variables.  
 165 The asterisks next to the squares denote the significant effects ( $p < 0.05$ ) of response function analyses.

166

设置了格式: 字体: 非加粗, 复杂文种字体: 非加粗



167



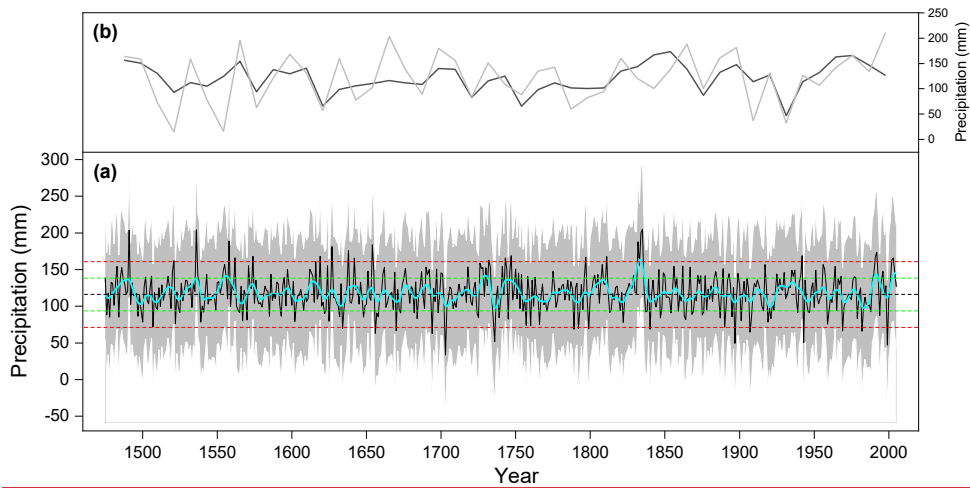
168

169 **Figure 54:** The moving correlation result between tree-ring width (TRW) chronology and non-growing season (NGS) precipitation during  
 170 the period of 1956–2005. The horizontal red and green dashed lines denote the significance levels of 0.05 and 0.01, respectively.

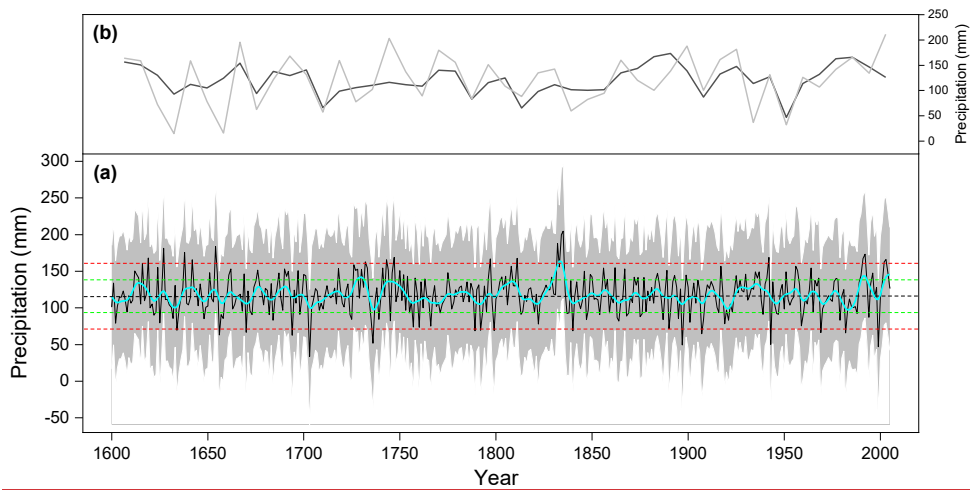
设置了格式: 字体: 非加粗, 复杂文种字体: 非加粗

171 **3.3 Non-growing season precipitation reconstruction**

172 According to the relationship between the TRW chronology and NGS precipitation, we developed a linear regression model  
 173 ( $y = 229.94x - 109.45$ ) and reconstructed the historical NGS precipitation series, which extended back to A.D. 1475–600  
 174 (Fig. 5a6a). In the model,  $y$  is the NGS precipitation, and  $x$  is the TRW index. The reconstruction accounted for 28.5% of the  
 175 instrumental NGS precipitation variability during the common time span (1956–2005). Figure 5b–6b shows the similarities  
 176 between the instrumental and reconstructed NGS precipitation series. We used a leave-one-out cross-verification method to  
 177 evaluate the legitimacy of the reconstruction model (Table 2). The positive RE and CE values (0.18 and 0.15, respectively)  
 178 were indicative of legitimacy of the reconstruction. The significant value (at 95%) of sign test implied that the model predicted  
 179 values were generally in line with the variation trend of instrumental values. In addition, the significant values of  $F$  test (at  
 180 99%) and PM test (at 95%) further confirmed the validity of the reconstruction. Overall, the statistics indicated that the  
 181 reconstruction model possessed good predictive skills.



182



183

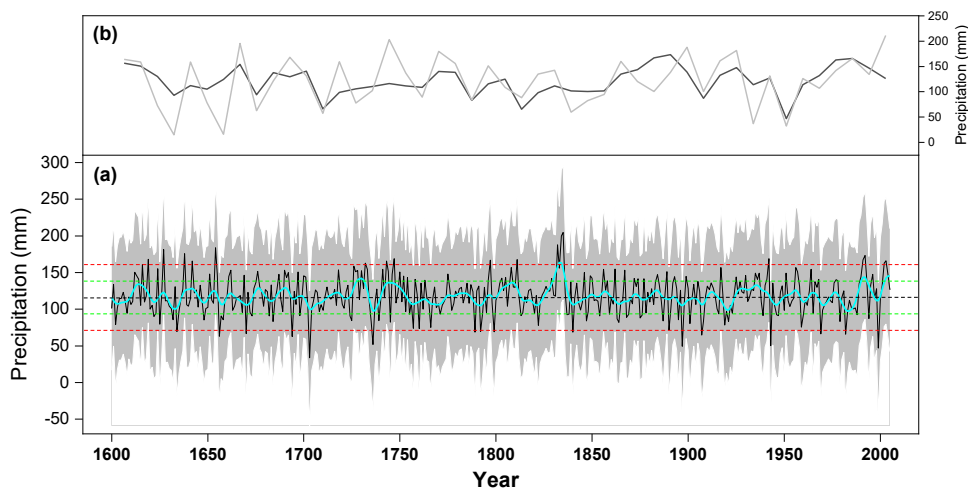


**Figure 65:** Non-growing season (NGS) precipitation reconstruction from A.D. 1475-1600 to 2005. (a). The black line is the reconstruction series, the thick cyan line is the 11-year loess smoothed result. The horizontal black dashed line is the mean of NGS precipitation value during from A.D. 1475-1600-2005. The horizontal green and red dashed lines are the one time and two times the of standard deviations of NGS precipitation, which indicated the boundaries for demonstrating demonstrated the boundaries of dry and extremely dry (below mean), and wet and extreme wet (above mean) years. The grey shading indicated the 95% confidence interval of the reconstruction; (b) Instrumental (black) and reconstructed (grey) NGS precipitation during their common period of 1956-2005.

设置了格式: 字体: 非加粗, 复杂文种字体: 非加粗

设置了格式: 字体: 非加粗, 复杂文种字体: 非加粗

设置了格式: 字体: 非加粗, 复杂文种字体: 非加粗

设置了格式: 字体: 非加粗, 复杂文种字体: 非加粗

**Table 2. Leave-one-out verification statistics for the non-growing season (NGS) precipitation reconstruction**

	$R$	$R^2$	$R_{adj}^2$	$F$	Sign-test	$Pmt$	$RE$	$CE$
Calibration	0.561	0.315	0.285	—	—	—	—	—
Verification	0.524	0.274	0.235	18.6**	36+/13- <sup>a</sup>	7.89*	0.18	0.15

格式化表格

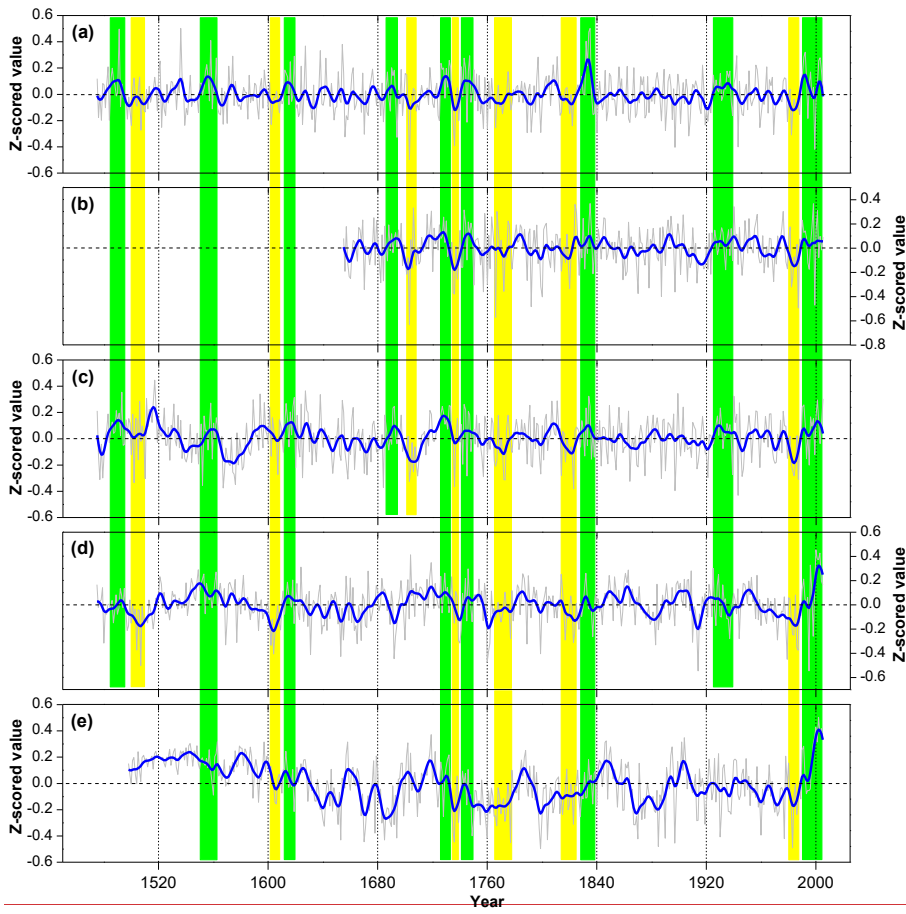
Note:  $R$  correlation coefficient,  $R^2$  explained variance,  $R_{adj}^2$  is the adjusted explained variance,  $F$   $F$ -test, Sign-test sign of paired observed and estimated departures from their mean on the basis of the number of agreements/disagreements,  $Pmt$  product mean test,  $RE$  reduction of error,  $CE$  coefficient of efficiency,  $DW$  Durbin-Watson test. \*  $p < 0.05$ , \*\*  $p < 0.01$

设置了格式: 字体: 非加粗, 复杂文种字体: 非加粗

198 **3.4 Characteristics of the NGS precipitation reconstruction**

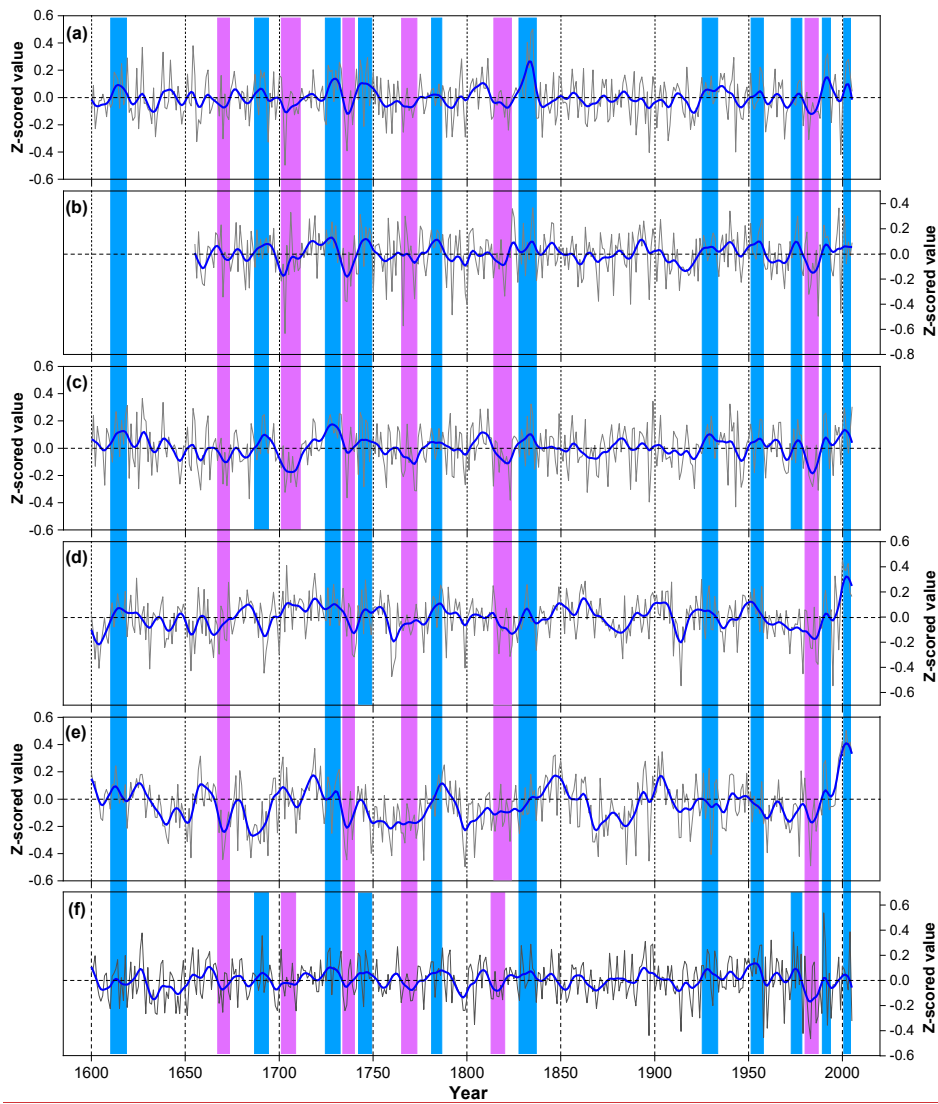
199 Figure [5a-6a](#) shows the reconstructed NGS precipitation over the past ~~531-406~~ years (A.D. ~~4475600~~-2005). The mean of the  
200 reconstructed NGS precipitation series was 118.25 mm, and the standard deviation (SD) was 25.22 mm. We pre-defined the  
201 years that had NGS precipitation below 93.03 mm (~~mean-SD~~) as dry NGS years, and below 67.81 mm (~~mean-2SD~~) as  
202 extremely dry years, whereas we defined years that had precipitation above 143.47 mm (~~mean+SD~~) as wet NGS years, and  
203 above 168.59 mm (~~mean+2SD~~) as extremely wet NGS years. Accordingly, the NGS was extremely dry during the years A.D.  
204 ~~1475~~, 1656, 1670, 1694, 1703, 1736, 1897, 1907, 1943, 1969, 1982, and 1999. In contrast, the NGS was extremely wet during  
205 the years A.D. ~~4491, 4536, 4558~~, 1627, 1638, 1654, 1832, 1834-1835, and 1992. The dry/wet ~~periods and some of the extreme~~  
206 ~~dry/wet~~ NGS periods in the present reconstruction were synchronised with dry/wet periods ~~and extreme dry/wet periods~~ in  
207 previously reported PDSI reconstruction from the surrounding region (Fig. [76](#), [Table S2](#), [Table S3](#)), ~~though some dissimilarities~~  
208 ~~were also existed~~. As shown in Fig. [78](#), the instrumental (a) and reconstructed (b) NGS precipitation series could represent the  
209 climatic conditions over a similar area in the SETP.

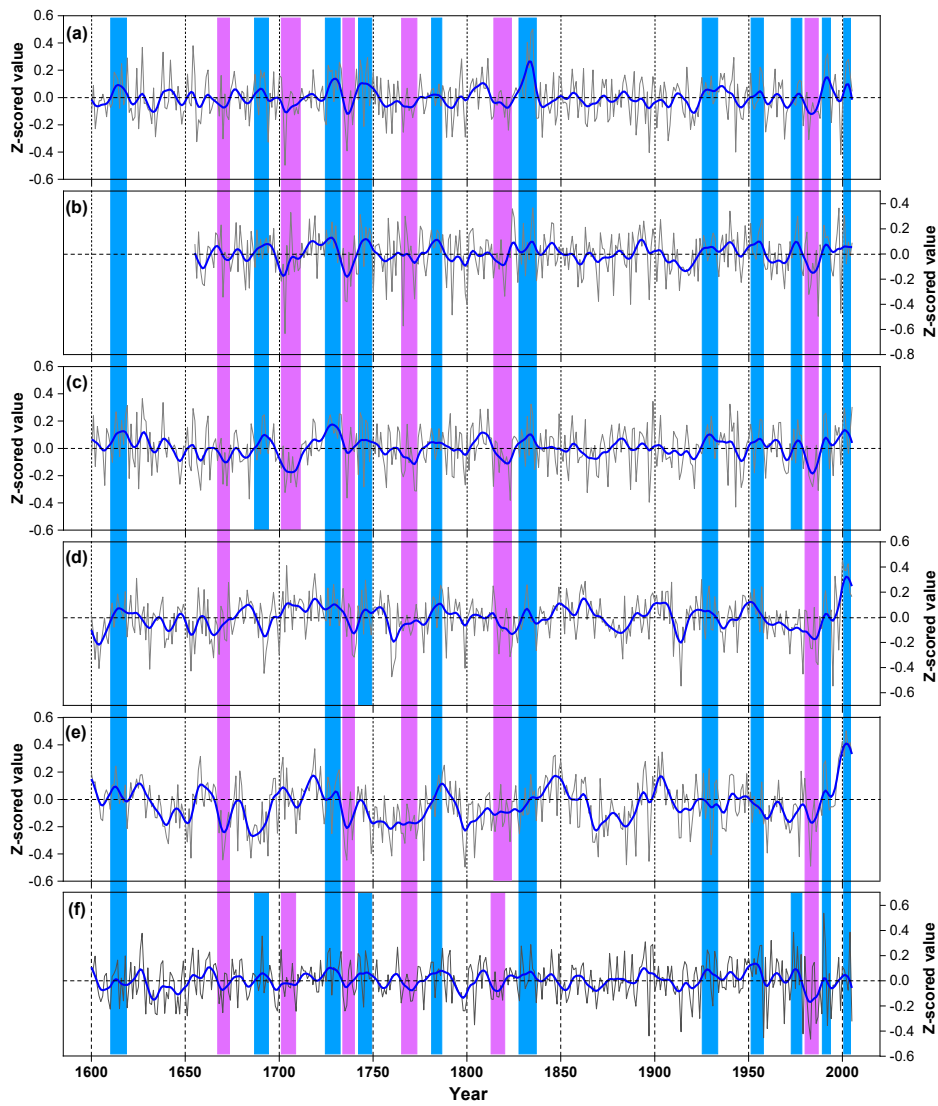




210

211

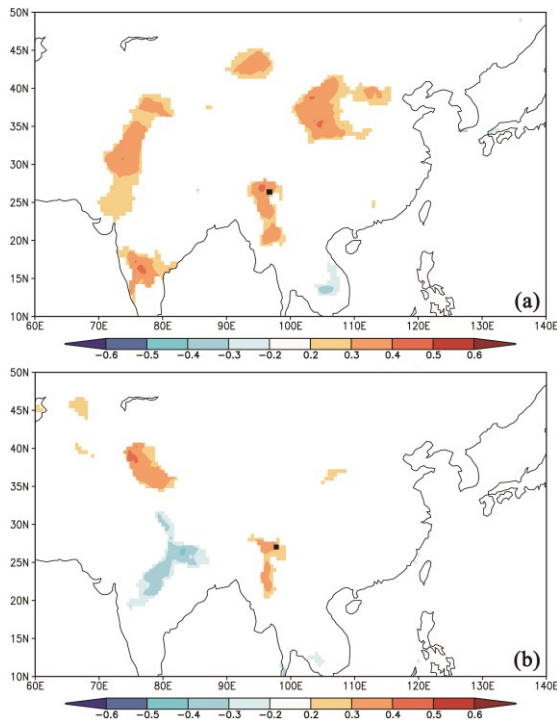




214 **Figure 76:** Comparisons of the hydroclimatic reconstructions in different studies. (a) The non-growing season (NGS)  
 215 precipitation reconstruction in the present study. (b) The current year March – May average Palmer Drought Severity Index  
 216 (PDSI) reconstruction in Fan et al. (2008). (c) The reconstruction of average PDSI from May of the previous year to April of  
 217 the current year in Fang et al. (2010). (d) The current year May-June average PDSI reconstruction in Zhang et al. (2015). (e)  
 218 The current year April-June average PDSI reconstruction in Li et al. (2017). (f) drought series extracted from Asian Monsoon  
 219 Atlas from the nearest point (Cook et al.2010). The blue green and yellow-purple bars show the common wet and dry periods  
 220 of the different reconstructions, respectively.

设置了格式: 字体: 非加粗, 复杂文种字体: 非加粗

设置了格式: 字体: 非加粗, 复杂文种字体: 非加粗  
 设置了格式: 字体: 非加粗, 复杂文种字体: 非加粗



222

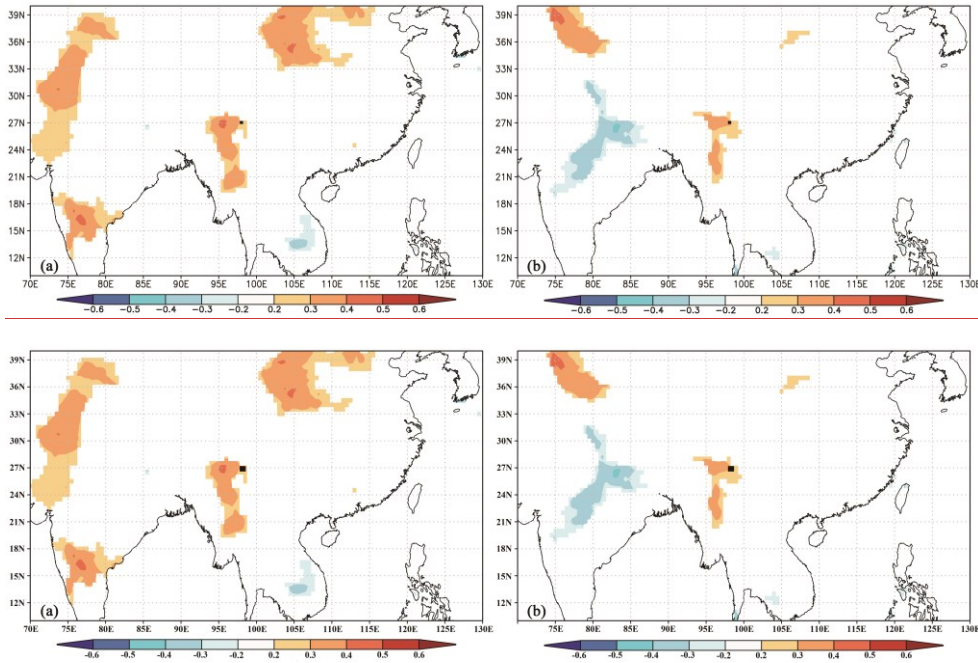


**Figure 87:** Spatial correlations between the actual (a) and reconstructed (b) non-growing season (NGS) precipitation and a gridded dataset of the NGS precipitation (average from November of the previous year to February of the current year) during their overlapping periods (1956–2005). The black square indicates the location of the study site.

设置了格式: 字体: 非加粗, 复杂文种字体: 非加粗

## 4. Discussion

### 4.1 Tree growth and climate relationship

The results of the tree growth and climate relationship analyses suggested that the forest hemlock radial growth in the northwestern Yunnan region of the SETP was strongly constrained by hydroclimatic factors. According to the Pearson correlation analysis, the influence of precipitation during the NGS on radial tree growth was greater than that of any other investigated climate variables and any correlation window. The response function analysis further confirmed the strong impact of NGS precipitation. In addition, the results of 32-year interval of moving correlation analysis (Fig. 45) suggested the

236 temporally consistent influence of NGS precipitation on forest hemlock radial growth in this region. The importance of NGS  
237 precipitation on the radial tree growth could be attributed to the fact that precipitation during the NGS compensated for the  
238 soil moisture, which was crucially important for supporting tree growth in the following season (Linderholm and Chen, 2005;  
239 Treydte et al. 2006; Wu et al., 2019; Li et al., 2021). This is because tree growth is often water stressed in the early stages of  
240 its growth in each year on the SETP when the monsoon precipitation does not arrive (Bräuning and Mantwill, 2004; Zhang et  
241 al., 2015), and the earlywood of tree rings mainly use spring melt water (Zhu et al., 2021). The eco-physiological importance  
242 of NGS precipitation on tree growth and tree water usage was also revealed by isotope ratios method-based investigations.  
243 Brinkmann et al's (2018) study showed that nearly 40% of the uptaken water by *Fagus sylvatica* and *Picea abies* trees in a  
244 temperate forest of middle Europe are sourced from NGS precipitation. Tree-ring oxygen isotope ratios ( $\delta^{18}O$ ) are  
245 demonstrated to contain NGS precipitation signals in the Himalayan region (Huang et al., 2019; Zhu et al., 2021). Huang et  
246 al's (2019) study revealed that NGS precipitation (snowfall) increased the snow-depth and the later snowmelt compensated  
247 soil moisture in the spring and early summer, which was a crucially important water source for the Juniper growth in the  
248 southwestern Tibetan Plateau. Zhu et al's (2021) investigation in the western Himalaya revealed that formation of earlywood  
249 in tree rings of *Pinus wallachina* depended on the snowmelt originated from NGS precipitation. The weak influence of  
250 precipitation on regional forest hemlock growth during March and April and strong influence during May was connected with  
251 the saddle-shaped monthly rainfall pattern of this area (Fig. 42). The correlations between precipitation and the TRW  
252 chronology were not significant during the growth-growing season (June-September) because an adequate water supply was  
253 available in the monsoon season.

254 Precipitation during the NGS over the SETP falls as snow. According to Sommerfeld et al. (1993) and Stadler et al. (1996),  
255 the development of a snowpack insulates the underlying soil from freezing temperatures, which creates unfrozen soil  
256 conditions and most of the soil processes that are active during warmer conditions also persist under snow cover, albeit at a  
257 reduced rate (Edwards, 2007). Unfrozen soil can reduce the cold and frost damage to the shallow root systems of conifer trees  
258 in this region (Schen and Jackson, 2002). A reduction in the cold damage to roots decreases the energy required to form new  
259 roots in the following growth year (Pederson et al., 2004), with the saved energy potentially used to initiate xylogenesis and  
260 form earlywood cells. Evergreen tree species are known to carry out year-round photosynthetic activity (Oquist and Huner,  
261 2003; Prats and Brodersen, 2020), albeit at a slower rate during the NGS, and therefore, the higher moisture availability  
262 contributes to the carbohydrate and energy accumulation process of forest hemlock in the investigation area.

263 In contrast, the radial tree growth was negatively correlated to temperature in most correlation windows (Fig. 24). This can  
264 be explained by the fact that higher temperature enhances evapotranspiration, and thus decreases water availability, which  
265 eventually constrains tree growth. The negative impact of NGS temperature on radial tree growth was obvious because the  
266 strengthened evaporation due to higher temperatures might reduce the moisture compensation to the soil layer and cause water  
267 stress during the early stage of the following growth season.

设置了格式: 字体: 倾斜, 复杂文种字体: 倾斜

设置了格式: 字体: 倾斜, 复杂文种字体: 倾斜

设置了格式: 字体: 倾斜, 复杂文种字体: 倾斜

#### 268 4.2 Validity of the reconstructed precipitation series

269 We have tried to validate the fidelity of the newly reconstructed series from different aspects. Although we used the residual  
270 TRW chronology in the present study, which removes autocorrelation (Cook and Kairiukstis, 1990) to capture the high  
271 frequency climate signals as in Fan et al. (2008) and Chen et al. (2016), the variability of dry and wet NGS at different scales  
272 was still retained in our reconstructed series. The reconstructed series in the present study demonstrated the variation in dry  
273 and wet NGS years (Fig. 56a). As in many other proxy based historical climate reconstruction studies, we compared our NGS  
274 precipitation series with other hydroclimatic reconstructions from the surrounding areas to investigate the reliability of our  
275 reconstruction. There are only countable numbers of hydroclimatic (PDSI) reconstructions in the nearby region, and not any  
276 case of precipitation reconstruction. Hence, we could only compare the present NGS precipitation reconstruction with existing  
277 PDSI reconstructions (Fig. 67). The compared PDSI reconstructions are of spring or early summer, because drought climate  
278 during these seasons usually associated with the winter precipitation, it makes certain sense to carry out the comparative  
279 analysis. The correlation coefficients between our NGS precipitation reconstruction and the PDSI reconstructions of Fan et al.  
280 (2008), Fang et al. (2010), Zhang et al. (2015) and Li et al. (2017) were 0.51 (n = 702), 0.35 (n = 1062), 0.25 (n = 1062) and  
281 0.22 (n = 1016) ( $p < 0.001$ ). We have extracted the drought series of Asian Monsoon Atlas (Cook et al.2010) from the nearest  
282 point to our investigation site and compared it with the NGS precipitation reconstruction in present study ( $R = 0.35$ , n = 1062,  
283  $p < 0.001$ ). As can be observed from Fig. 76, there were dry and wet periods in compared reconstruction series which were  
284 consistent with the NGS precipitation variabilities. These similarities indicated the reliability of our NGS precipitation  
285 reconstruction to some extent. The correlation coefficients for the present reconstruction with those of Fan et al. (2008) and  
286 Fang et al. (2010) were greater than those with Li et al. (2017) and Zhang et al. (2015). These differences were probably due  
287 to the different distances among the study sites. Although, the major dry and wet periods were similar in the hydroclimatic  
288 reconstructions referenced above, there were still certain discrepancies in duration and the strength of the dry/wet climatic  
289 conditions. This is probably because of the differences in the types of hydro-climatic variables (precipitation, PDSI), specific  
290 seasons reconstructed (annual, seasonal), ~~the different~~ tree species (species with different drought tolerances), ~~different~~  
291 chronology recording methods (standard chronology, residual chronology), length of calibration period, sample replication  
292 and the geomorphic differences of the tree-ring sampling sites (altitude, slope) (Table S1).

293 In addition, we uploaded both of the instrumental and reconstructed NGS precipitation data for the same period of 1956–  
294 2005 on the KNMI website and conducted a spatial correlation analyses with the CRU gridded climate dataset. The similar  
295 patterns of spatial correlation between the instrumental and reconstructed dataset (Fig. 78) indicated that the present  
296 reconstruction was reliable and could represent the NGS precipitation over a large area of the SETP. Besides, the occurrence  
297 of some historical great drought events in the Asian monsoon area (Cook et al., 2010, Kang et al., 2013), i.e., the 1756–1768  
298 (strange parallels drought), 1790, 1792–1796 (east India drought) and 1920s (~~post-World War I China mega-~~drought), matched  
299 the dry NGS periods in our reconstruction, which also further confirmed the reliability of our reconstruction.

设置了格式: 字体: 倾斜, 复杂文种字体: 倾斜

设置了格式: 字体: 倾斜, 复杂文种字体: 倾斜

300 It should be noted that the lower sample replication prior to 1600 resulted in a reduced EPS, with a value below the commonly  
301 used threshold value of 0.85 in tree-ring based climate reconstruction studies. This may affect the reliability of the  
302 reconstruction before 1600. We therefore suggest caution in the interpretation of the reconstructed NGS precipitation series  
303 prior to the 17<sup>th</sup> century. Nevertheless, we found similarities between the wet/dry NGS conditions before A.D. 1600 in our  
304 reconstructed series and those of Fang et al. (2010) and Zhang et al. (2015) from the surrounding area (Fig. 6).

## 305 5. Conclusion

306 In this study, we investigated ~~534~~<sup>406</sup> years of residual TRW chronology of forest hemlock in the SETP, China. The climate  
307 and tree growth relationship ~~analysis~~<sup>analyses</sup> showed that the TRW chronology was mostly negatively correlated with the  
308 thermal variable (temperature), whereas it was positively correlated with hydroclimatic variables (precipitation ~~and PDSI~~ <sup>and</sup>  
309 <sup>PDSI</sup>, indicating that hydroclimatic conditions determined the radial growth of forest hemlock in this region. Accordingly, we  
310 derived a linear model of the relationship between climate and tree growth, which accounted for 28.5% of the actual NGS  
311 precipitation variance (1956–2005), and we used the model to reconstruct the historical (A.D. ~~1475~~<sup>1600</sup>–2005) NGS  
312 precipitation. The reconstructed series showed that the NGS was extremely dry during the years A.D. ~~1475~~, 1656, 1670, 1694,  
313 1703, 1736, 1897, 1907, 1943, 1969, 1982 and 1999. In contrast, the NGS was extremely wet during the years A.D. ~~1491~~,  
314 ~~1536~~, ~~1558~~, 1627, 1638, 1654, 1832, 1834–1835 and 1992. A comparison between the NGS precipitation reconstruction in  
315 this study and PDSI reconstructions from nearby regions revealed a coherency in the timing of dry and wet episodes, suggesting  
316 the reliability of our reconstruction.

317 **Data availability.** The climate reconstruction series in this study can be obtained from Zongshan Li after the paper publication.

318 **Author contributions.** ZSL and MK conceived the study; ZSL, ZXF, XCW collected the tree-ring data; MK, ZSL, ZXF, KYF,  
319 XCW elaborated the methodology; MK, ZSL, WLC analysed the data; MK, ZSL led the writing of the manuscript; ZSL and  
320 ZXF revised the manuscript; BJF and GHL validated the final manuscript.

321 **Competing interests.** The authors declare that they have no conflict of interest.

322 **Acknowledgement.** This work was funded by the National Key Research Development Program of China (2016YFC0502105),  
323 the second Tibetan Plateau Scientific Expedition and Research (STEP) Program (2019QZKK0502). We are grateful to the  
324 editor and anonymous reviewers for their valuable comments and suggestions to improve this article.

## 325 References

326 Biondi, F. and Waikul, K.: DENDROCLIM2002: a C++ program for statistical calibration of climate signals in tree ring  
327 chronologies, *Comput. Geosci.*, 30(3), 303-311, <https://doi.org/10.1016/j.cageo.2003.11.004>, 2004



328 Bräuning, A. and Mantwill, B.: Summer temperature and summer monsoon history on the Tibetan Plateau during the last 400  
329 years recorded by tree rings, *Geophys. Res. Lett.*, 31, L24205, <https://doi.org/10.1029/2004GL020793>, 2004

330 Bunn, A. G. and Korpela, M.: An introduction to dplR. The Comprehensive R Archive Network,  
331 <https://cran.biodisk.org/web/packages/dplR/vignettes/intro-dplR.pdf>, 2018

332 Büntgen, U., Mygland, V. S., Ljungqvist, F. C., McCormick, M., Di Cosmo N., Sigl, M., Jungclauss, J., Wagner, S., Krusic, P.  
333 J., Esper, J., Kaplan, J. O., de Vaan MAC., Luterbacher, J., Wacker, L., Tegel, W. and Kirilyanov, A. V.: Cooling and societal  
334 change during the Late Antique Little Ice Age from 536 to around 660 AD, *Nat. Geosci.*, 9, 231–236,  
335 <https://doi.org/10.1038/ngeo2652>, 2016

336 Büntgen, U., Tegel, W., Nicolussi, K., McCormick, M., Frank, D., Trouet, V., Kaplan, J. O., Herzig, F., Heussner, K. U.,  
337 Wanner, H., Luterbacher, J. and Esper, J.: 2500 years of European climate variability and human susceptibility, *Science*, 331,  
338 578–582, <https://doi.org/10.1126/science.1197175>, 2011

339 Cai, Q. F., Liu, Y., Lei, Y., Bao, G. and Sun, B.: Reconstruction of the march-august PDSI since 1703 AD based on tree rings  
340 of Chinese pine (*Pinus tabulaeformis* Carr.) in the Lingkong Mountain, southeast Chinese loess Plateau, *Clim. Past.*, 10, 509–  
341 521, <https://doi.org/10.5194/cp-10-509-2014>, 2014

342 Chen, F., Yuan, Y. J., Zhang, T. W., Shang, H.: Precipitation reconstruction for the northwestern Chinese Altay since 1760  
343 indicates the drought signals of the northern part of inner Asia, *Int. J. Biometeorol.*, 60(3), 455-463.  
344 <https://doi.org/10.1007/s00484-015-1043-5>, 2016

345 Cook, E. R. and Kairiukstis, A.: *Methods of Dendrochronology: Applications in the Environmental Sciences*, Kluwer  
346 Academic Press, Dordrecht, 1990

347 Cook, E. R., Anchukaitis, K. J., Buckley, B. M., D'Arrigo, R. D., Jacoby, G. C. and Wright, W. E.: Asian monsoon failure and  
348 megadrought during the last millennium, *Science*, 328(5977), 486-489, <https://doi.org/10.1126/science.1185188>, 2010

349 Cook, E. R., Briffa, K. R., Meko, D. M., Graybill, D. A. and Funkhouser, G.: The 'segment length curse' in long tree-ring  
350 chronology development for palaeoclimatic studies, *Holocene*, 5(2), 229-237. <https://doi.org/10.1177/095968369500500211>,  
351 1995

352 D'Arrigo, R. D., Mashig, E., Frank, D. C., Wilson, R. J. S. and Jacoby, G. C.: Temperature variability over the past millennium  
353 inferred from Northwestern Alaska tree rings, *Clim. Dyn.*, 24, 227-236. <https://doi.org/10.1007/s00382-004-0502-1>, 2005

354 Duan, K., Yao, T. and Thompson, L.: Response of monsoon precipitation in the Himalayas to global warming, *J. Geophys.*  
355 *Res.*, 111, D19110. <https://doi.org/10.1029/2006JD007084>, 2006

356 Edwards, A. C., Scalenghe, R., Freppaz, M.: Changes in the seasonal snow cover of alpine regions and its effect on soil  
357 processes: a review. *Quat. Int.*, 162-163, 172-181. <https://doi.org/10.1016/j.quaint.2006.10.027>, 2007

358 Esper, J.: 1300 years of climatic history for Western Central Asia inferred from tree-rings, *Holocene*, 12(3), 267-277.  
359 <https://org.doi.10.1191/0959683602hl543rp>, 2002

360 Fan, Z. X., Bräuning, A. and Cao, K. F.: Tree-ring based drought reconstruction in the central Hengduan Mountains region  
361 (China) since AD 1655, *Int. J. Climatol.*, 28, 1879–1887, <https://doi.org/10.1002/joc.1689>, 2008

362 Fan, Z. X., Bräuning, A., Yang, B. and Cao, K. F.: Tree ring density-based summer temperature reconstruction for the central  
363 Hengduan Mountains in southern China, *Glob. Planet. Change*, 65 (1-2), 1-11.  
364 <https://doi.org/10.1016/j.gloplacha.2008.10.001>, 2009

365 Fang, K. Y., Gou, X. H., Chen, F., Li, J. B., D'Arrigo, R., Cook, E. D., Yang, T. and Davi, N.: Reconstructed droughts for the  
366 southeastern Tibetan Plateau over the past 568 years and its linkages to the Pacific and Atlantic Ocean climate variability,  
367 *Clim. Dyn.*, 35(4), 577–585. <https://doi.org/10.1007/s00382-009-0636-2>, 2010

368 Fritts, H. C., Guiot, J. and Gordon, G. A.: Verification. In: Cook E and Kairiukstis LA, eds., *Methods of Dendrochronology: Applications in the Environmental Sciences*. Dordrecht, Kluwer Academic Publishers, 178-184, 1990

370 Fritts, H. C.: *Tree rings and climate*. Academic Press, London, 1976

371 Griessinger, J., Bräuning, A., Helle, G., Hochreuther, P. and Schleser, G.: Late Holocene relative humidity history on the  
372 southeastern Tibetan plateau inferred from a tree ring  $\delta^{18}O$  record: recent decrease and conditions during the last 1500 years,  
373 *Quat. Int.*, 430, 52–59, <http://dx.doi.org/10.1016/j.quaint.2016.02.011>, 2017

374 He, H. M., Bräuning, A., Griessinger, J., Hochreuther, P. and Wernicke, J.: May–June drought reconstruction over the past  
375 821 years on the southcentral Tibetan Plateau derived from tree-ring width series, *Dendrochronologia*, 47, 48–57,  
376 <https://doi.org/10.1016/j.dendro.2017.12.006>, 2018

377 He, H. M., Yang, B., Bräuning, A., Wang, J. L. and Wang, Z. Y.: Tree-ring derived millennial precipitation record for the  
378 south-central Tibetan plateau and its possible driving mechanism, *Holocene*, 23 (1), 36-45,  
379 <https://doi.org/10.1177/0959683612450198>, 2012

380 Holmes, R. L.: Computer-assisted quality control in tree-ring dating and measurement, *Tree-ring Bulletin*, 43, 69-75, 1983

381 Huang, R., Zhu, H. F., Liang, E. Y., Liu, B., Shi, J. F., Zhang, R. B., Yuan, Y. J., Griessinger, J.: A tree ring-based winter  
382 temperature reconstruction for the southeastern Tibetan Plateau since 1340 CE, *Clim. Dyn.*, 53, 3221-3233.  
383 <https://doi.org/10.1007/s00382-019-04695-3>, 2019

384 [Kang, S. Y., Bao, Y., Qin, C., Wang, J. L., Feng, S., Liu, J. J.: Extreme drought events in the years 1877–1878, and 1928, in the southeast Qilian mountains and the air-sea coupling system. \*Quat. Intern.\*, 283\(427\), 85-92. <https://doi.org/10.1016/j.quaint.2012.03.011>, 2013](https://doi.org/10.1016/j.quaint.2012.03.011)

387 Keyimu, M., Li, Z. S., Liu, G. H., Fu, B. J., Fan, Z. X., Wang, X. C. Zhang, Y. D., Halik, U.: Tree-ring based minimum  
388 temperature reconstruction on the southeastern Tibetan Plateau, *Quat. Sci. Rev.*, 251, 106712.  
389 <https://doi.org/10.1016/j.quascirev.2020.106712>, 2021

390 Keyimu, M., Wei, J. S., Zhang, Y. X., Zhang, S., Li, Z. S., Ma, K. M., Fu, B. J.: Climate signal shift under the influence of  
391 prevailing climate warming – Evidence from *Quercus liaotungensis* on Dongling Mountain, Beijing, China,  
392 *Dendrochronologia*, 60, 125683. <https://doi.org/10.1016/j.dendro.2020.125683>, 2020

393 Li, J. B., Shi, J. F., Zhang, D. D., Yang, B., Fang, K. Y. and Yue, P. H.: Moisture increase in response to high-altitude warming  
394 evidenced by tree-rings on the southeastern Tibetan Plateau, *Clim. Dyn.*, 48, 649–660. [https://doi.org/10.1007/s00382-016-](https://doi.org/10.1007/s00382-016-3101-z)  
395 [3101-z](https://doi.org/10.1007/s00382-016-3101-z), 2017

396 Li, T., Li, J.B.: A 564-year annual minimum temperature reconstruction for the east central Tibetan Plateau from tree rings,  
397 *Glob. Planet. Change*, 157, 165-173. <https://doi.org/10.1016/j.gloplacha.2017.08.018>, 2017.

398 Li, Z. S., Zhang, Q. B. and Ma, K. P.: Tree-ring reconstruction of summer temperature for A.D. 1475–2003 in the central  
399 Hengduan Mountains, northwestern Yunnan, China, *Clim. Change*, 110(1-2), 455-467, [https://doi.org/10.1007/s10584-011-](https://doi.org/10.1007/s10584-011-0111-z)  
400 [0111-z](https://doi.org/10.1007/s10584-011-0111-z), 2011

401 *Liang, E. Y., Liu, X. H., Yuan, Y. J., Qin, N. S., Fang, X. Q., Huang, L., Zhu, H. F., Wang, L. L. and Shao, X. M.: The 1920s*  
402 *drought reconstructed by tree rings and historical documents in the semi-arid and arid areas of northern China, Clim. Change,*  
403 *79, 403–432. https://doi.org/10.1007/s10584-006-9082-x, 2006*

404 Linderholm, H. W., Chen, D.: Central Scandinavian winter precipitation variability during the past five centuries reconstructed  
405 from *Pinus sylvestris* tree rings, *Boreas*, 34, 43–52, 2005

406 Michaelsen, J.: Crossevalidation in statistical climate forecast models, *J Clim. App. Meteorol.*, 26, 1589-1600, 1987

407 R: A language and environment for statistical computing. R Foundation for Statistical Computing, Vienna, Austria. URL  
408 <https://www.R-project.org/>, 2020<sup>19</sup>

409 Oquist, G., Huner, N. P.: Photosynthesis of overwintering evergreen plants, *Annu. Rev. Plant Biol.*, 54, 329–355.  
410 <https://doi.org/10.1146/annurev.arplant.54.072402.115741>, 2003

411 Prats, K. A., Brodersen, C. R.: Seasonal coordination of leaf hydraulics and gas exchange in a wintergreen fern, *AoB Plants*,  
412 12(6), 1–13. <https://doi.org/10.1093/aobpla/plaa048>, 2020

413 Pederson, N., Cook, E. R., Jacoby, G. C., Peteet, D. M., Griffin, K. L.: The influence of winter temperatures on the annual  
414 radial growth of six northern range margin tree species, *Dendrochronologia* 22 (1), 7–29.  
415 <https://doi.org/10.1016/j.dendro.2004.09.005>, 2004

416 Rangwala, I., Miller, J. R. and Xu, M.: Warming in the Tibetan Plateau: Possible influences of the changes in surface water  
417 vapor, *Geophys. Res. Lett.*, 36, L06703, <https://doi.org/10.1029/2009GL037245>, 2009

418 Schenk, H. J., & Jackson, R. B.: The global biogeography of roots. *Ecol. Monogr*, 72, 311–328. [https://doi.org/10.1890/0012-9615\(2002\)072\[0311:TGBOR\]2.0.CO;2](https://doi.org/10.1890/0012-9615(2002)072[0311:TGBOR]2.0.CO;2), 2002

420 Schneider, L., Smerdon, J. E., Büntgen, U., Wilson, R. J. S., Myglan, V. S., Kirilyanov, A. V. and Esper, J.: Revising mid-latitude summer temperatures back to AD 600 based on a wood density network, *Geophys. Res. Lett.*, 42, 4556–4562. <https://doi.org/10.1002/2015GL063956>, 2015

423 Shi, C. M., Sun, C., Wu, G. C., Wu, X. C., Chen, D. L., Masson-Delmotte, V., Li, J. P., Xue, J. Q., Li, Z. S., Ji, D. Y., Zhang, J., Fan, Z. X., Shen, M. G., Shu, L. F., Ciais, P.: Summer temperature over Tibetan Plateau modulated by Atlantic multi-decadal variability, *J. Clim.*, 32, 4055–4067. <https://doi.org/10.1175/JCLI-D-17-0858.1>, 2019

426 Shi, S. Y., Li, J. B., Shi, J. F., Zhao, Y. S. and Huang, G.: Three centuries of winter temperature change on the southeastern Tibetan plateau and its relationship with the Atlantic Multidecadal Oscillation, *Clim. Dynam.*, 49, 1305–1319. <https://doi.org/10.1007/s00382-016-3381-3>, 2017

429 Sommerfeld, R. A., Mosier, A. R., Musselman, R. C.: CO<sub>2</sub>, CH<sub>4</sub> and N<sub>2</sub>O flux through a Wyoming snowpack and implications for global budget, *Nature*, 361, 140–142, <https://doi.org/10.1038/361140a0>, 1993

431 Stadler, D., Wunderli, H., Auckenthaler, A., Fluhler, H.: Measurement of frost induced snowmelt runoff in a forest soil, *Hydrol. Process.*, 10, 1293–1304, [https://doi.org/10.1002/\(SICI\)1099-1085\(199610\)10:10<1293::AID-HYP461>3.0.CO;2-I](https://doi.org/10.1002/(SICI)1099-1085(199610)10:10<1293::AID-HYP461>3.0.CO;2-I), 1996

433 Wang, J. L., Yang, B., Ljungqvist, F. C.: A millennial summer temperature reconstruction for the eastern Tibetan Plateau from tree-ring width, *J. Clim.*, 28(13), 5289–5304. <https://doi.org/10.1175/JCLI-D-14-00738.1>, 2015

435 [Wernicke, J., Griessinger, J., Hochreuther, P., Bräuning, A.: Variability of summer humidity during the past 800 years on the eastern Tibetan plateau inferred from  \$\delta^{18}O\$  of tree-ring cellulose. \*Clim. Past\*, 10\(4\), 3327–3356. <https://doi.org/10.5194/cp-11-327-2015>. 2015](https://doi.org/10.1002/2015GL063956)

438 Wigley, T. M., Briffa, K. R., and Jones, P. D.: On the average value of correlated time series, with applications in dendroclimatology and hydrometeorology, *J. Clim. Appl. Meteorol.*, 23, 201–213, [https://doi.org/10.1175/1520-0450\(1984\)0232.0.CO;2](https://doi.org/10.1175/1520-0450(1984)0232.0.CO;2), 1984

441 Wilson, R., Anchukaitis, K., Briffa, K. R., Büntgen, U., Cook, E., D'Arrigo, R., Davi, N., Esper, J., Frank, D., Gunnarson, B., Hegerl, G., Helama, S., Klesse, S., Krusic, P.J., Linderholm, H.W., Myglan, V., Osborn, T.J., Rydval, M., Schneider, L., Schurer, A., Wiles, G., Zhang, P. and Zorita, E.: Last millennium northern hemisphere summer temperatures from tree rings: Part I: the long term context, *Quat. Sci. Rev.*, 134, 1–18. <https://doi.org/10.1016/j.quascirev.2015.12.00>, 2016

445 Wu, G., Duan, A., Liu, Y., Mao, J., Ren, R., Bao, Q., He, B., Liu, B. and Hu, W.: Tibetan Plateau climate dynamics: recent research progress and outlook, *Natl. Sci. Rev.*, 2, 100–116, <https://doi.org/10.1093/nsr/nwu045>, 2015

447 Wu, X. C., Li, X. Y., Liu, H. Y., Ciais, P., Li, Y. Q., Xu, C. Y., Babst, F., Guo, W. C., Hao, B. Y., Wang, P., Huang, Y. M.,  
448 Liu, S. M., Tian, Y. H., He, B. and Zhang, C. C.: Uneven winter snow influence on tree growth across temperate China, *Glob.*  
449 *Change Biol.*, 25, 144–154. <https://doi.org/10.1111/gcb.14464>, 2019

450 Yan, L. and Liu, X.: Has climatic warming over the Tibetan Plateau paused or continued in recent years? *J. Earth Ocean Atmos.*  
451 *Sci.*, 1, 13–28, 2014

452 Yang, B., Qin, C., Wang, J., He, M., Melvin, T. M., Osborn, T. J.: A 3,500-year tree-ring record of annual precipitation on the  
453 northeastern Tibetan Plateau, *Proc. Natl. Acad. Sci. U. S. A.*, 111(8), 2903-2908. <https://doi.org/10.1073/pnas.1319238111>,  
454 2014

455 Zhang, Q. B., Evans, M. N., Lyu, L. X.: Moisture dipole over the Tibetan Plateau during the past five and a half centuries, *Nat.*  
456 *Commun.*, 6, 8062. <https://doi.org/10.1038/ncomms9062>, 2015

457 [Zhu, H. F., Huang, R., Asad, F., Liang, E. Y., Bräuning, A., Zhang, X. Z., Dawadi, B., Man, W. M., Griessinger, J.: Unexpected](#)  
458 [climate variability inferred from a 380-year tree-ring earlywood oxygen isotope record in the Karakoram, Northern Pakistan,](#)  
459 [Clim. Dynam., https://doi.org/10.1007/s00382-021-05736-6, 2021](#)